RSC Advances

COMMUNICATION

View Article Online
View Journal | View Issue

CrossMark click for updates

Cite this: *RSC Adv.*, 2014, **4**, 43024

Received 25th July 2014
Accepted 28th August 2014

DOI: 10.1039/c4ra07593e

www.rsc.org/advances

Published on 28 August 2014. Downloaded by Michigan State University on 20/01/2016 10:03:38.

# Facile synthesis of self-assembled mesoporous CuO nanospheres and hollow $Cu_2O$ microspheres with excellent adsorption performance†

Siyuan Yang,[a] Shengsen Zhang,[ab] Hongjuan Wang,[a] Hao Yu,[a] Yueping Fang[b] and Feng Peng*[a]

Self-assembled mesoporous CuO nanospheres (CuO NSs) and hollow $Cu_2O$ microspheres ($Cu_2O$ MSs) were synthesized by a facile ethylene glycol–water solvothermal method without any surfactants. The formation and evolution of copper oxides were investigated by controlling the synthesis conditions. The as-prepared $Cu_xO$ materials showed an excellent adsorption capability for the quick removal of Acid Orange 7 (AO7) dye in water.

As important functional materials, copper ($Cu^+$ or $Cu^{2+}$) oxides have been widely investigated in recent years, since they are inexpensive, environmentally benign, non-toxic and abundant.[1–4] Copper oxide (CuO and $Cu_2O$), typically, has potential applications in the field of solar energy conversion, adsorption, photo-degradation, electronics, and gas sensors.[5–8] In our previous reports, it was reported that porous nano-size $Cu_2O$ nanoparticles have a selective adsorption property for anionic dyes, showing a new potential application of $Cu_xO$ in removing anionic dyes from waste water for environment treatment.[9,10] It is well known that nanomaterials with spontaneous assembly and hierarchical structures show a strong correlation between their function and geometry.[11] Therefore, porous semiconductor materials endowed with a large number of reaction sites, high specific surface area, high specific strength and good permeability are particularly significant in the practical applications.

Recently, considerable research efforts have been undertaken to develop simple methods for the fabrication of low-dimensional copper oxide semiconductor materials. Yang's group have exploited the concept of nanostructures engineering on copper foil surface through a solution chemical route.[12] They have synthesized a series of copper-based materials on the surface of pure copper foil, such as CuO nanorods arrays and $Cu_2O$ nanowires arrays.[13,14] It have also been demonstrated that the crystal structure transformation among Cu, CuO and $Cu_2O$ is practicable.[15–17] As a more facile synthesis route, alcohol-based reduction method has been widely used to synthesize copper oxide materials. For example, Guo's group synthesized $Cu_2O$/GO and CuO/GO composite *via* a diethylene glycol reduction method which exhibited enhanced photoelectrocatalytic activity.[18,19] However, capping agent is usually indispensable in order to achieve satisfactory diversified structures. At present, capping agent or surface active agent, such as polyvinylpyrrolidone (PVP), cetyltrimethylammonium bromide (CTAB) and sodium dodecyl sulfate (SDS), were widely investigated to purposefully synthesize $Cu_2O$ nanocubes,[20–22] multi-shelled $Cu_2O$ (ref. 23 and 24) and multi-aspect $Cu_2O$ spheres.[25–27] To obtain morphology-controllable and crystal-assignable copper oxide materials, complex experimental steps, strict reaction conditions and toxic reduction agent are often required. So far, among different methods reported for copper oxide nanocrystals, it is worth mentioning that a simple and suitable method for preparing porous copper oxide is still unsatisfactory. Therefore, it is necessary to develop a facile method to fabricate copper oxide with controllable structure.

In the current work, a simple water–ethylene glycol (EG) mixed solvothermal route for the formation of mesoporous CuO nanospheres (NSs) and hollow microspheres $Cu_2O$ (MSs) has been investigated. The uniform and size controllable CuO NSs could be obtained *via* a spontaneous aggregation and crystallization processes in the absence of any surfactants or additives (even pH adjusting agency of NaOH). With the assistant of glucose, hollow $Cu_2O$ MSs could be easily received. The possible growth process of CuO NSs nanocrystal was detected by investigating the relationship between the morphology changes and the growth temperatures. It was also found that, with the addition of reduction agent (glucose), the reaction temperature has strong influence on the final $Cu_2O$ size-distribution and homogeneity. Finally, selective adsorption performances of the synthesized samples were also investigated. It was found that

[a]*School of Chemistry and Chemical Engineering, South China University of Technology, Guangzhou, Guangdong, 510640, China. E-mail: cefpeng@scut.edu.cn; Fax: +86 20 87114916; Tel: +86 20 87114916*

[b]*College of Science, South China Agricultural University, Guangzhou, 510642, China*

† Electronic supplementary information (ESI) available: Experimental details and supplementary figures. See DOI: 10.1039/c4ra07593e



This journal is © The Royal Society of Chemistry 2014

Published on 28 August 2014. Downloaded by Michigan State University on 20/01/2016 10:03:38.

the as-prepared CuO NSs have a large BET specific surface area (around 168 $m^2$ $g^{-1}$) and show an excellent adsorption capability in the removal of AO7 dye from water.

Mesoporous CuO NSs were synthesized by a simple solvothermal route without the presence of any other reagent addition. In a standard synthesis, 10 ml of copper acetate ($Cu(Ac)_2$, 0.1 M), 5 ml of $H_2O$ and 45 ml of ethylene glycol (EG) were mixed to form a solution in a round-bottom flask (100 ml), the homogeneous mixed solution was then put into an 160 °C oil bath and stirred under reflux for one hour. Varied reaction temperatures were performed to investigate the spontaneous aggregation and crystallization processes of CuO NSs. The process for $Cu_2O$ MSs synthesis was basically as the same as that of CuO NSs except that 5 ml glucose solution (0.43 M) was injected into the initial mixed solution before the solvothermal reaction, $Cu_2O$ MSs with different size distributions can be obtained at different reaction temperatures. The final black CuO NSs and reddish-yellow $Cu_2O$ MSs were collected by centrifugation and washed with water and ethanol for several times to remove most of the EG. Two kinds of $Cu_2O$ crystals with different morphology were also obtained by a controlled glucose added manner, which were denoted as $Cu_2O$ polyhedron and $Cu_2O$ cube (see ESI, Experiment section and Fig. S1–S2†).

The nanostructure transformation of the CuO NSs and $Cu_2O$ MSs were examined by SEM, TEM and XRD. It is found that the reaction temperature is a crucial condition for the growth of copper oxides crystals in the EG reduction progress, which affects the morphology and constructions of copper oxides. A group of typical SEM imagines of CuO NSs obtained at different reaction temperatures are presented in Fig. 1, which clearly shows the growth procedure of the products. At a relative low temperature (80 °C), after 1 h reaction, the light blue mixed solution turned to olive green, which indicated the formation of irregular CuO nanoparticles (Fig. 1A). Uniform spindle-shaped CuO nanorods with sharp ends formed from tiny nanosheets spontaneously assembled at a little higher reaction temperature of 100 °C (Fig. 1B). When the reaction temperature was improved to 140 °C, small amounts of CuO NSs appeared (Fig. 1C). With the temperature of 160 °C, the nearly monodisperse nanospheres formed in large scale as shown in Fig. 1D and E. The corresponding TEM imagine is given in Fig. 1F. The mean CuO NSs size was determined by randomly selecting 500 CuO NPs from Fig. 1E. It is found that the average diameter of CuO NSs is 412 nm and the histogram of the size distribution is inserted in Fig. 1E. Looking carefully at the feature of samples from the four different reaction temperature periods, it is conclude that: (i) the final monodispersed mesoporous CuO NSs with wavy-like surface (sample in Fig. 1D) are composed of many self-assembly schistose CuO (samples in Fig. 1A–C), and (ii) the reaction temperature obviously influences the final morphology of CuO and a higher temperature could effectively enhance the aggregation of CuO piece-like crystallites; the higher reaction temperature is favorable for the more uniform crystallite size distribution of CuO NSs.

When glucose as a reduction agency was injected into the original mixed solution ($H_2O$–EG–$Cu(Ac)_2$) in the solvothermal reaction, $Cu_2O$ microspheres could be achieved. Based on the examination of the reaction temperature-dependent formation of CuO NSs, the $Cu_2O$ MSs at different reaction temperatures were also synthesized. As can be seen from Fig. 2A–D, All of the synthesized samples at the reaction temperature from 60 to

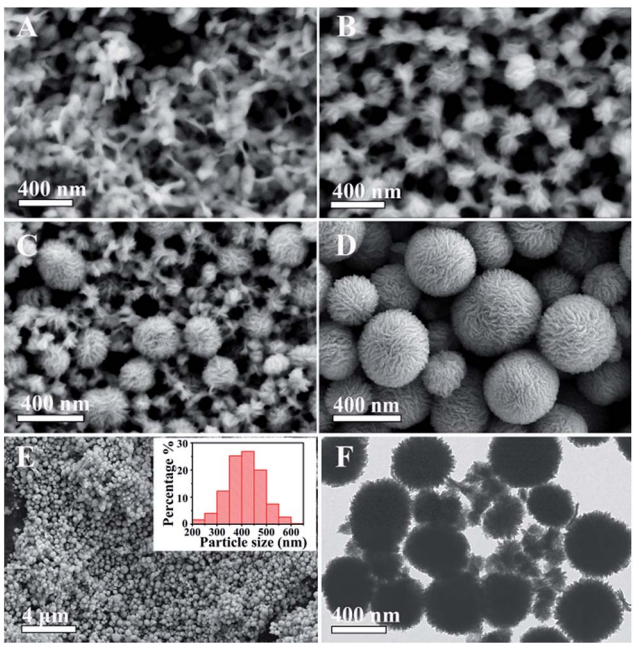


Fig. 1 The morphological transformation of synthesized CuO NSs at different reaction temperatures of 80 °C (A), 100 °C (B), 140 °C (C) and 160 °C (D and E). (F) is the corresponding TEM imagines of (D). The inset in (E) is a histogram of the size distribution from the as synthesized CuO NSs.

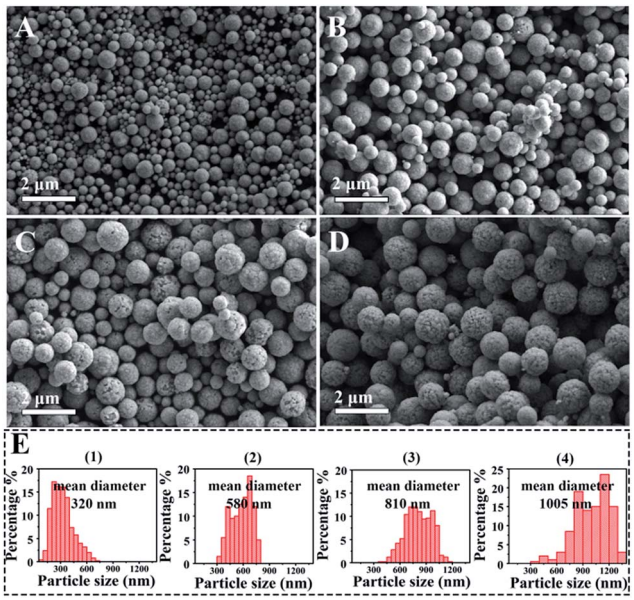


Fig. 2 SEM images of $Cu_2O$ samples obtained at different synthesis temperatures of 60 °C (A), 80 °C (B), 100 °C (C) and 140 °C (D). E is the corresponding size distribution histogram calculated for A, B, C and D samples.

Published on 28 August 2014. Downloaded by Michigan State University on 20/01/2016 10:03:38.

140 °C have sphere structures. With the increase of reaction temperature, the average diameter of the spheres increases and the spheres become more homogeneous. Fig. 2E(1)–(4) are the corresponding size distribution histograms calculated from samples in Fig. 2A–D, which clearly reveals that the mean diameter increases from 320 nm to 1 μm.

A very homogeneous and completely monodispersed $Cu_2O$ MSs were obtained at a higher reaction temperature of 160 °C. The morphology and hierarchical porous structure of the as-prepared $Cu_2O$ MSs were observed by SEM. Fig. 3A–C show SEM images of the as-synthesized $Cu_2O$ MSs at different magnifications, it is can be seen from Fig. 3A that bulk quantities of $Cu_2O$ MSs were fabricated with relatively uniform diameters. A histogram of the size distribution of the $Cu_2O$ is shown as inset in Fig. 3A. It is found that the diameters of $Cu_2O$ MSs are in the range of from 0.9 to 2.1 μm and the mean diameter is 1.5 μm. Fig. 3B–C reveal that these monodisperse $Cu_2O$ MSs have a hollow spherical structure with the shell thickness of about 400 nm. More interestingly, there are a lot of mesoporous in the $Cu_2O$ MSs shell walls (Fig. 3D), which proves that the as-synthesized $Cu_2O$ MSs are composed of center hollow monodispersed microspheres with abundant mesoporous on the wall. We speculate that the reduction effect of glucose led to the formation of $Cu_2O$ hollow structure. Especially, in higher reaction temperature of 160 °C, glucose was decomposed to produce carbon dioxide gas, resulting in the prominent hollow structure.

The crystal structure of all the final obtained samples was verified by XRD. Fig. 4 shows the XRD patterns for both the CuO NSs and $Cu_2O$ MSs received at 160 °C. From Fig. 4a and b, it can be see that all the diffraction peaks for CuO NSs and $Cu_2O$ MSs can be readily indexed to the monoclinic symmetry of CuO (JCPDS 45-0937) and face-centred cubic $Cu_2O$ (JCPDS 05-0667), respectively. No obvious impurities were detected, indicating the purity of the synthesized samples.

As it is known to all, the size and morphology of nanomaterials have a great effect on their chemical and physical properties and therefore their applications. The synthesized

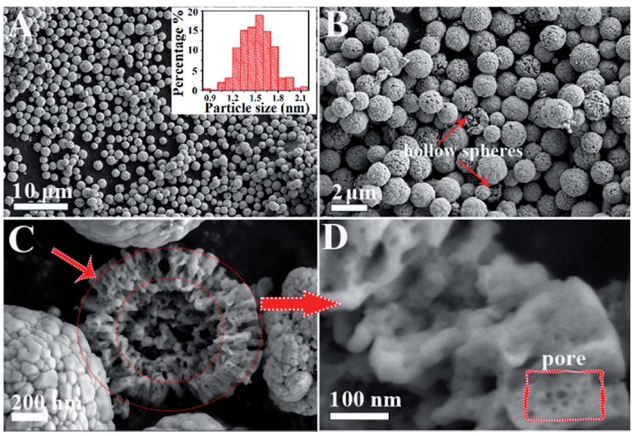


Fig. 3 SEM images with different magnifications of the as-synthesized $Cu_2O$ MSs at the synthesis temperature of 160 °C.

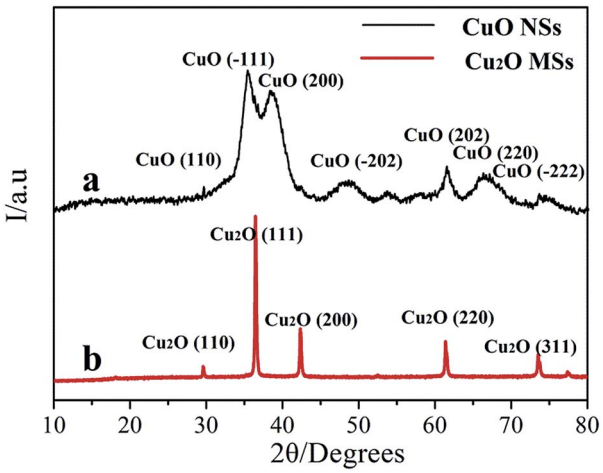


Fig. 4 XRD patterns of the CuO NSs (a) and $Cu_2O$ MSs (b) respectively.

$Cu_xO$ materials with different morphology were employed as efficient adsorbents to effectively remove dyes from water and thus could be used for the environment treatment. For comparison, the adsorptive capability of commercial CuO (c-CuO) and $Cu_2O$ (c-$Cu_2O$) were also investigated. Adsorption performances of all samples were assessed with AO7, methyl orange (MO) and methyl blue (MB). The results showed the as-synthesized $Cu_xO$ nanostructures had a highly selective adsorption characteristic for anionic dyes MO and AO7, especially AO7, but no adsorption was observed for cationic dye MB (see ESI, Table S1 and Fig. S3†). The zeta potential of the synthesized CuO NSs and $Cu_2O$ MSs samples were measured to be +31 mV and +28 mV, respectively. The positive zeta potential of $Cu_xO$ surfaces have also been found in our previous reports.[10] Here, we presume the mechanism of selective adsorption can be attributed to the electrostatic adsorptions. The absorption kinetics of the CuO NSs and $Cu_2O$ MSs received at 160 °C for AO7 is shown in Fig. 5A. It can be seen that all the synthesized materials arrived adsorptive equilibrium within 30 min. CuO NSs can rapidly remove AO7 over 97.5% in 15 min, at the same time, $Cu_2O$ MSs also reach 60.7%. Both of them are much higher removal rate than the commercial CuO and $Cu_2O$, which only have a low removal rate for AO7 (5.2% and 11.4%,

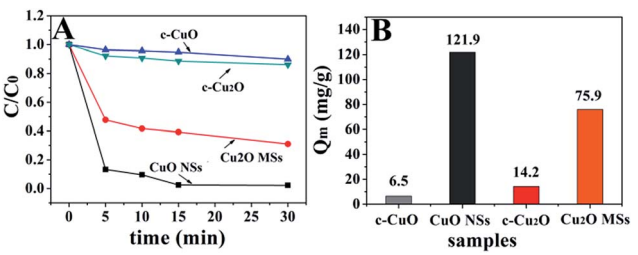


Fig. 5 (A) Adsorption kinetics of the as prepared $Cu_xO$ materials (20 mg) and the commercial CuO and $Cu_2O$ (20 mg) for AO7 (50 mg $L^{-1}$). $C_0$ is the initial concentration of AO7 solution and $C$ is the concentration of AO7 in the solution at different adsorption time. (B) Adsorption capacity of all the samples for AO7.


This journal is © The Royal Society of Chemistry 2014

Published on 28 August 2014. Downloaded by Michigan State University on 20/01/2016 10:03:38.

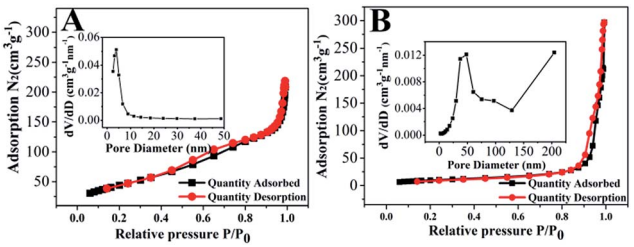


Fig. 6 (A) and (B) $N_2$ adsorption curves of the as-obtained CuO NSs and $Cu_2O$ MSs; the inset shows the pore size distribution for the two samples respectively.

respectively). The adsorption capacity of $Cu_xO$ were further calculated from the statistical chart of AO7 adsorption in 15 min. Fig. 5B apparently shows that the as-synthesized CuO NSs and $Cu_2O$ MSs samples both have higher adsorption capacities for AO7 dye, which are almost 20 times and 5 times those of commercial CuO and $Cu_2O$, respectively. To test the reusability of copper oxides particles (CuO NSs and $Cu_2O$ MSs) for dye adsorption, we carried out the bleaching experiment for AO7 repeatedly five times. As shown in Fig. S4,† the reactivated samples can quickly adsorb AO7 from the contaminative solution every time and the adsorption performances are not significantly weakened. These results further proved that the as-synthesized CuO NSs and $Cu_2O$ MSs are effective and stable for quickly removal of AO7 dye in water.

The mechanism of selective adsorption had been demonstrated in our previous report, which was mainly attributed to the electrostatic adsorption.[10] In fact, the porous structure of the as-synthesized CuO NSs and $Cu_2O$ MSs may affect the adsorption capacity and rate. Herein, the $N_2$ adsorption/desorption isotherms and pore size distributions of CuO NSs and $Cu_2O$ MSs were tested. As show in Fig. 6A and B, the BET surface areas of the two samples are 168.2 and 36.5 $m^2\ g^{-1}$ for CuO NSs and $Cu_2O$, respectively, which are far larger than those of c-CuO (5.1 $m^2\ g^{-1}$) and c-$Cu_2O$ (3.2 $m^2\ g^{-1}$). The insets in Fig. 6A and B show that the pore-size distribution centres are at 5 nm for CuO NSs and 50 nm for $Cu_2O$ MSs. In addition, the large pores (diameter > 150 nm) in the $Cu_2O$ sample can be attributed to the centre hollow structure in $Cu_2O$ MSs, as shown in the Fig. 3C. All these results are matched well with the SEM and TEM images. The effectively enhancement of the adsorption capacity mainly is attributed to the increase of surface physical adsorption active sites on the $Cu_xO$ spheres, which are supplied by the porous structure. This study has developed a facile and practical pathway for the preparing $Cu_xO$ porous materials, which are promising and interesting for potential applications of anionic dyes adsorption from waste water quickly.

## Conclusions

The uniform and size controllable CuO NSs and $Cu_2O$ MSs can be obtained *via* a spontaneous aggregation and crystallization processes in the absence of any surfactants or additives. The growth progress and conditions were studied in detail by controlling the reaction temperature; the as-prepared $Cu_xO$ materials show excellent adsorption capability for the quick removal of AO7 dye in water.

## Acknowledgements

This work was supported by the financial support from the National Natural Science Foundation of China (no. 20873044), the Guangdong Provincial Science and Technology Project of China (2011B B050400014) and the China Postdoctoral Science Foundation (no. 2012M521606; 2014T70808).

## Notes and references

1 G. Ghadimkhani, N. R. de Tacconi, W. Chanmanee, C. Janaky and K. Rajeshwar, *Chem. Commun.*, 2013, **49**, 1297–1299.
2 K. Chen, S. Song and D. Xue, *CrystEngComm*, 2013, **15**, 144.
3 X. Jiang, T. Herricks and Y. Xia, *Nano Lett.*, 2002, **2**, 1333–1338.
4 P. Wang, Y. H. Ng and R. Amal, *Nanoscale*, 2013, **5**, 2952–2958.
5 D. Barreca, P. Fornasiero, A. Gasparotto, V. Gombac, C. Maccato, T. Montini and E. Tondello, *ChemSusChem*, 2009, **2**, 230–233.
6 L. Zhang, J. Shi, M. Liu, D. Jing and L. Guo, *Chem. Commun.*, 2014, **50**, 192–194.
7 J. Zhang, J. Liu, Q. Peng, X. Wang and Y. Li, *Chem. Mater.*, 2006, **18**, 867–871.
8 W. Wang, O. K. Varghese, C. Ruan, M. Paulose and C. A. Grimes, *J. Mater. Res.*, 2011, **18**, 2756–2759.
9 L. Huang, F. Peng, H. Yu and H. Wang, *Solid State Sci.*, 2009, **11**, 129–138.
10 L. Huang, F. Peng, H. Yu and H. Wang, *Mater. Res. Bull.*, 2008, **43**, 3047–3053.
11 G. R. Bourret and R. B. Lennox, *J. Am. Chem. Soc.*, 2010, **132**, 6657–6659.
12 W. Zhang, X. Wen and S. Yang, *Inorg. Chem.*, 2003, **42**, 5005–5014.
13 S. Anandan, X. Wen and S. Yang, *Mater. Chem. Phys.*, 2005, **93**, 35–40.
14 X. Wen, Y. Xie, C. L. Choi, K. C. Wan, X.-Y. Li and S. Yang, *Langmuir*, 2005, **21**, 4729–4737.
15 W. T. Yao, S. H. Yu, Y. Zhou, J. Jiang, Q. S. Wu, L. Zhang and J. Jiang, *J. Phys. Chem. B*, 2005, **109**, 14011–14016.
16 J. Y. Xiang, J. P. Tu, X. H. Huang and Y. Z. Yang, *J. Solid State Electrochem.*, 2007, **12**, 941–945.
17 S. Glaus and G. Calzaferri, *Photochem. Photobiol. Sci.*, 2003, **2**, 398.
18 X. Guo, C. Hao, G. Jin, H. Y. Zhu and X. Y. Guo, *Angew. Chem., Int. Ed.*, 2014, **53**, 1973–1977.
19 X. Y. Yan, X. L. Tong, Y. F. Zhang, X. D. Han, Y. Y. Wang, G. Q. Jin, Y. Qin and X. Y. Guo, *Chem. Commun.*, 2012, **48**, 1892–1894.
20 J. C. Park, J. Kim, H. Kwon and H. Song, *Adv. Mater.*, 2009, **21**, 803–807.

21 M. H. Kim, B. Lim, E. P. Lee and Y. Xia, *J. Mater. Chem.*, 2008, **18**, 4069.
22 C. Lu, L. Qi, J. Yang, X. Wang, D. Zhang, J. Xie and J. Ma, *Adv. Mater.*, 2005, **17**, 2562–2567.
23 W. Wang, Y. Tu, P. Zhang and G. Zhang, *CrystEngComm*, 2011, **13**, 1838.
24 H. Xu and W. Wang, *Angew. Chem., Int. Ed.*, 2007, **46**, 1489–1492.
25 C.-H. Kuo and M. H. Huang, *J. Phys. Chem. C*, 2008, **112**, 18355–18360.
26 M. Cao, C. Hu, Y. Wang, Y. Guo, C. Guo and E. Wang, *Chem. Commun.*, 2003, **39**, 1884–1885.
27 C. H. Kuo, C. H. Chen and M. H. Huang, *Adv. Funct. Mater.*, 2007, **17**, 3773–3780.

Published on 28 August 2014. Downloaded by Michigan State University on 20/01/2016 10:03:38.


This journal is © The Royal Society of Chemistry 2014